

Generalized Quantum Mechanical Two-Centre Problems

III. Calculation of Exact Expectation Values*

KLAUS HELFRICH

Institute and Centre of Theoretical Chemistry
University of Frankfurt a. Main

Received June 2, 1970

If $\chi_i(\chi_k)$ is an exact generalized diatomic orbital (solution of Eq. (1) of text), a sequence of functions $\chi_i^{(N)}$ converging to χ_i may be constructed so that matrix elements of frequently occurring operators between $\chi_i^{(N)}$ and $\chi_k^{(N)}$ may be computed without any numerical integration. Exact expectation values are given for kinetic and potential energy, dipole moment, $\rho^2 = x^2 + y^2$, and quadrupole moment $3z^2 - r^2$, for various ratios of nuclear charges Z_1, Z_2 and for several distances R . Special subjects discussed in terms of computed expectation values are:

- i) R -dependence of the contributions to total energy of HeH^{2+} in state $2p\sigma$ and of LiH^{3+} in state $3d\sigma$
- ii) RZ - and λ -dependence of dipole and quadrupole moment functions in state $1s\sigma$
- iii) Some properties of those generalized diatomic orbitals which approach, for R going to 0, Slater-type atomic functions.

Sei $\chi_i(\chi_k)$ eine exakte Lösung des verallgemeinerten Zweizentren-Problems (Gl. (1) im Text). Dann lässt sich eine Funktionenfolge $\chi_i^{(N)}$ konstruieren, die gegen χ_i konvergiert und so beschaffen ist, daß Matrixelemente häufig benötigter Operatoren zwischen $\chi_i^{(N)}$ und $\chi_k^{(N)}$ ohne numerische Integrationen berechnet werden können. Exakte Erwartungswerte werden für kinetische und potentielle Energie, Dipolmoment, $\rho^2 = x^2 + y^2$ und Quadrupolmoment $3z^2 - r^2$ für zahlreiche Kombinationen von Kernladungszahlen Z_1, Z_2 und verschiedene Kernabstände angegeben.

Von berechneten Erwartungswerten ausgehend, werden insbesondere diskutiert:

- 1) die R -Abhängigkeit der Energiebestandteile von HeH^{2+} im Zustand $2p\sigma$ und von LiH^{3+} im Zustand $3d\sigma$
- 2) Die RZ - und λ -Abhängigkeit der Dipol- und Quadrupolmomentfunktion im $1s\sigma$ -Zustand
- 3) einige Eigenschaften solcher verallgemeinerter zweiatomiger Orbitale, die für $R \rightarrow 0$ gegen atomare Slaterfunktionen konvergieren.

Si $\chi_i(\chi_k)$ est une orbitale diatomique généralisée exacte (solution de l'équation (1)), on peut construire une suite de fonctions $\chi_i^{(N)}$ convergent vers S_i , telle que les éléments de matrice des opérateurs courants entre $\chi_i^{(N)}$ et $\chi_k^{(N)}$ puissent être calculés sans aucune intégration numérique. Les valeurs moyennes exactes sont obtenues pour l'énergie cinétique et l'énergie potentielle, le moment dipolaire, $\rho^2 = x^2 + y^2$ ainsi que le moment quadrupolaire $3z^2 - r^2$ pour différents rapports des charges nucléaires Z_1, Z_2 et différentes distances R .

On discute des sujets suivants en fonction des valeurs moyennes calculées:

- 1) variations avec R des contributions à l'énergie pour HeH^{2+} dans l'état $2p\sigma$ et LiH^{3+} dans l'état $3d\sigma$.
- 2) variations avec RZ et λ des moments dipolaires et quadrupolaires dans l'état $1s\sigma$.
- 3) certaines propriétés de ces orbitales diatomiques généralisées qui, lorsque R tend vers zéro, se rapprochent des fonctions atomiques de type Slater.

* Part of this was delivered on the Seminar on Computational Problems in Quantum Chemistry, Straßburg 1969.

A. Introduction

In previous work ([1], from now on referenced by I) on the separable generalized quantum mechanical two-centre problem

$$\left(-\frac{A}{2} - \frac{Z_1}{r_1} - \frac{Z_2}{r_2} - \frac{Q}{r_1 \cdot r_2} \right) \chi = E \chi, \quad (1)$$

emphasis was put on the exact computation of the energy E and the separation constant A' (I, Eq. (5a) and (5b)) as functions of R , RZ_1 , RZ_2 , and Q for various electronic states.

There are several reasons for now making available expectation values, computed with χ .

i) Not only H_2^+ in the $1s\sigma_g$ state, but also HeH^{2+} ($2p\sigma$) and LiH^{3+} ($3d\sigma$) possess each a total energy curve with a minimum. The question is whether the discussion of the chemical binding in H_2^+ given by Slater (for instance in [2]) further holds when heteronuclear one-electron systems are considered.

ii) Increasing work is done on nuclear charge expansions for the energy and other properties of diatomic molecules so that our results may serve as test values or as a numerical basis.

iii) Recent own CI-calculations on two- and four-electron-molecules show the necessity of including those functions of type (1) which converge to Slater type atomic orbitals (STAOs) for $R \rightarrow 0$ in the one-electron basis. Some properties of these "Slater type diatomic orbitals" (STDOS) are to be studied.

B. Method of Generating $\chi^{(N)}$ and of Computing Matrix Elements

I. In order to get approximations $\chi^{(N)}$ with $\lim_{N \rightarrow \infty} \chi^{(N)} = \chi$ (solution of (1)) possessing such a form that the calculation of matrix elements becomes easy, the following procedure consisting of three steps has been successfully applied:

In the *first step*, the energy parameter p , defined by

$$E = -\frac{2p^2}{R^2}, \quad (2)$$

and the separation constant A' , defined by Eq. (5) of I, are determined simultaneously by a Newton-Raphson-procedure for two variables which has been described in I and [3]. It is essentially based on *three-term* recursion formulas for the expansion coefficients. Table 1 contains the underlying expansions for the factors $U(\mu)$ and $V(v)$ of χ .

In the *second step*, an expansion for $V(v)$ used in the first step is cast away (if $Z_1 \neq Z_2$) in favour of an expansion in terms of generalized Legendre functions without a factor $\exp(\pm pv)$. This new expansion gives rise to a *five-term* recursion formula for the expansion coefficients. As p and A' are known, at that stage of computation, with high accuracy, two steps of Wieland iteration

$$(\mathbf{B} + A' \mathbf{E}) \mathbf{d}'^{(n+1)} = \mathbf{d}'^{(n)} \quad (n = 0, 1) \quad (3)$$

will do to determine the expansion coefficients d'_k gathered in the column vector \mathbf{d}' . The pentadiagonal matrix \mathbf{B} is given in the appendix; the numerical method for treating (3) is due to Zurmühl [4].

In the case $Z_1 = Z_2 (D_{\infty h})$ and if the coefficients c'_k for $U(\mu)$ are to be computed, Miller's recurrence algorithm [5] provides a stable and fast procedure for solving

$$\mathbf{A} \mathbf{c}' = -\mathbf{A}' \mathbf{c}' \quad (4)$$

with \mathbf{A} a tridiagonal matrix (I).

In the *third and last step*, the expansions of $U(\mu)$ and $V(v)$ are truncated to $N_c + 1$ respectively $N_d + 1$ terms, usually choosing $N_c + 1 = N_d + 1 = N$. The finite expansions in terms of polynomials $L_{|m|+j}^{(ml)}(2pt)$ and $P_{|m|+k}^{(ml)}(v)$ are transformed into equivalent ordinary polynomials in terms of powers of $t = \mu - 1$ and of v , using formulae given by Miller [6]. After normalization, the final computational form of $\chi^{(N)}$ is

$$\chi^{(N)} = \sqrt{\frac{8}{R^3}} e^{-pt} \sum_{j=0}^{N_c} c_j t^j [t(t+2)(1-v^2)]^{\frac{|m|}{2}} \sum_{k=0}^{N_d} d_k v^k \frac{e^{im\varphi}}{\sqrt{2\pi}} \quad (4a)$$

$$t = \mu - 1 \quad (4b)$$

$$(\chi^{(N)} | \chi^{(N)}) = 1 \quad (4c)$$

$$\int_{-1}^1 \left[[1-v^2]^{\frac{|m|}{2}} \sum_{k=0}^{N_d} d_k v^k \right]^2 dv = 1$$

All three steps are contained in the body of the ALGOL procedure GENDO. Its input parameters are the quantum numbers n, l, m , and the quantities RZ_1, RZ_2, Q, N ; output is $p, m, N_c, \mathbf{c}, N_d, \mathbf{d}$.

II. \mathbf{F} be a multiplicative operator representable by a finite polynomial in the two variables $t = \mu - 1$ and v :

$$(\mu^2 - v^2) \mathbf{F} = \sum_i \sum_k a_{ik} t^i v^k. \quad (5)$$

Evidently \mathbf{F} is well described by the matrix \mathbf{a} with elements a_{ik} . For computing

$$F_{pq}^{(N)} = (\chi_p^{(N)} | \mathbf{F} | \chi_q^{(N)}), \quad (6)$$

which is done by a call of the ALGOL procedure MATRIXELEMENT, only polynomial multiplications and calculation of integrals such as

$$\int_0^\infty e^{-pt} t^j dt = \frac{j!}{P^{j+1}} \quad (\text{no } A\text{-integrals!}) \quad (7a)$$

$$\int_{-1}^1 v^j dv = \begin{cases} 0 & j \text{ odd} \\ \frac{2}{j+1} & j \text{ even} \end{cases} \quad (\text{no } B\text{-integrals!}) \quad (7b)$$

have to be performed.

Table 1. Suggested expansions and corresponding algorithms for generalized diatomic orbitals

$$\chi^{(N)} = \sqrt{\frac{8}{R^3}} U(\mu) V(v) \frac{e^{im\phi}}{\sqrt{2\pi}}$$

	$U(\mu)$	$V(v)$
1st step: Evaluation of p, A'	$e^{-\frac{x}{2}} (\mu^2 - 1)^{\frac{ m }{2}} \sum_{j=0}^{\infty} c'_j L_{ m +j}^{ m }(x)$ with $x = 2p(\mu - 1)$	$\sum_{k=0}^{\infty} d'_k P_{ m +k}^{ m }(v)$ if $Z_1 = Z_2$ (DIORPA)
Algorithm: Newton-Raphson- procedure for 2 variables		
2nd step: generation of $\chi^{(N)}$	as above	$\sum_{k=0}^{k_{\max}} d'_k P_{ m +k}^{ m }(v)$
Algorithms:	Miller's recurrence algorithm	Wielandt iteration if $Z_1 \neq Z_2$ Miller's rec. alg. if $Z_1 = Z_2$
3rd step: transformation of $\chi^{(N)}$ into computational form	$e^{-pt} [t(t+2)]^{\frac{ m }{2}} \sum_{j=0}^{N_c} c_j t^j$ with $t = \mu - 1$	$[1 - v^2]^{\frac{ m }{2}} \sum_{k=0}^{N_d} d_k v^k$

Operators representable in the form (5) are, for instance

$$\begin{aligned} \frac{1}{r_1} &= \frac{2}{R(\mu + v)} & \frac{1}{r_2} &= \frac{2}{R(\mu - v)} & \frac{1}{r_1 r_2} &= \frac{4}{R^2(\mu^2 - v^2)} \\ z &= \frac{R}{2} \mu v & \varrho^2 &= \frac{1}{4} (\mu^2 - 1)(1 - v^2) \end{aligned} \tag{8}$$

The matrix element of the kinetic energy $-A/2$ between two functions of the form (4) can be evaluated by several calls of MATRIXELEMENT (T2).

III. In order to compute

$$F_{pq} = (\chi_p | F | \chi_q) \tag{9}$$

between exact solutions χ_p, χ_q of (1), the sequence

$$F_{pq}^{(N)} = (\chi_p^{(N)} | F | \chi_q^{(N)}) \tag{10}$$

has to be studied.

The following numerical example shows the speed of convergence of $F^{(N)}$ to the expectation value of $F = \varrho^2 = x^2 + y^2$ for the $1s\sigma_g$ state of H_2^+ . Graphs of ϱ^2 and $\bar{T} = -A/2$, as functions of R , computed for various states of $H_2^+(Z_1 = Z_2 = 1)$

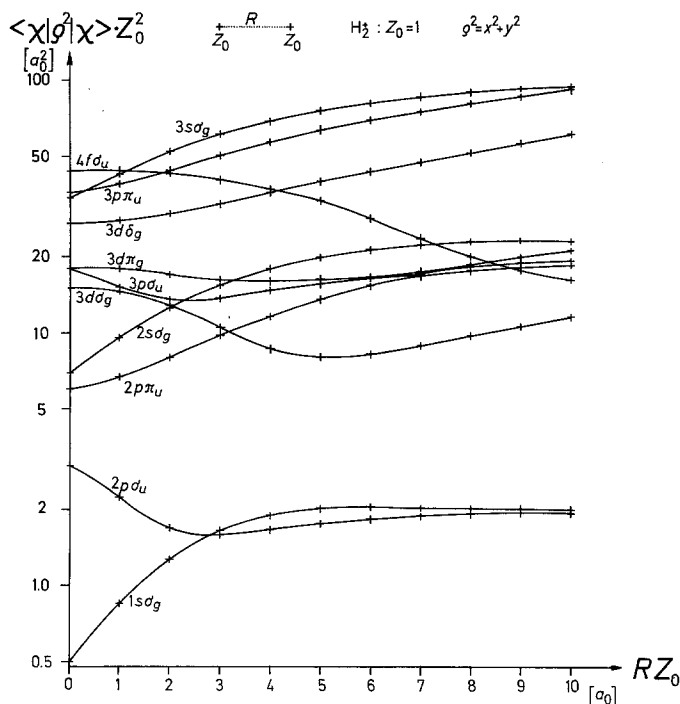


Fig. 1. Expectation values $\langle \chi | \rho^2 \rangle$ of the square of the distance between the electron and the internuclear axis as functions of the nuclear distance R , for 11 states of H_2^+

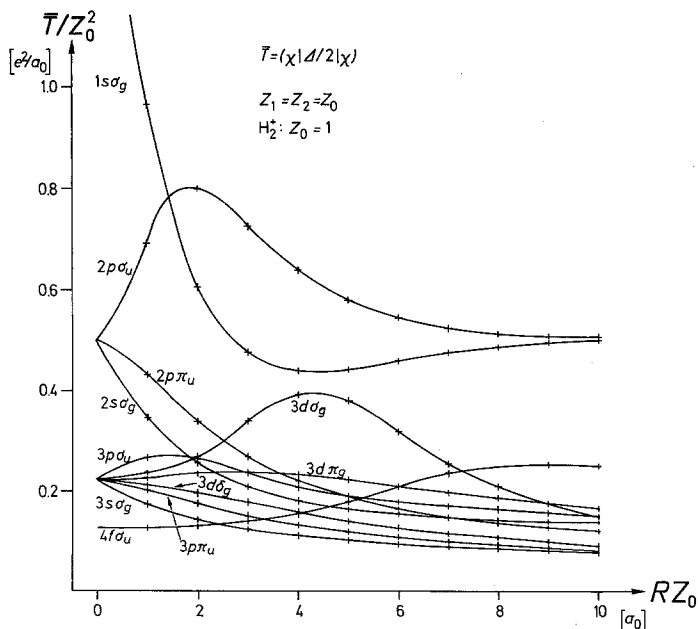


Fig. 2. Expectation values of kinetic energy as functions of the nuclear distance R , for 11 states of H_2^+

and other homonuclear one-electron molecules ($Z_1 = Z_2 = Z_0 \neq 1$), are given in Figs. 1 and 2.

N	$R = 1a_0$	$R = 2a_0$	$R = 5a_0$	$R = 10a_0$
3	0.844642	1.28218	2.03610	2.01720
4	0.847234	1.28351	2.03653	2.00559
5	0.847056	1.28345	2.03652	2.00610
6	0.847055	1.28345	2.03652	2.00611
7	0.847054	1.28345	2.03652	2.00611
8	0.847054	1.28345	2.03652	2.00611

C. R -Dependence of the Contributions to the Total Energy in the $2p\sigma$ State of HeH^{2+} and in the $3d\sigma$ State of LiH^{3+}

In [2], Slater has examined the ground state $1s\sigma_g$ of H_2^+ and given a thorough analysis of the behaviour of expectation values

$$\begin{aligned}\overline{E_{\text{kin}}} &= (\chi | -A/2 | \chi) \\ \overline{E_{\text{pot}}} &= \left(\chi \left| -\frac{Z_0}{r_1} - \frac{Z_0}{r_2} \right| \chi \right) + \frac{Z_0^2}{R} \\ E_{\text{tot}} &= \overline{E_{\text{kin}}} + \overline{E_{\text{pot}}}\end{aligned}\quad (11)$$

as functions of the internuclear distance R .

Since it has been known that also the system HeH^{2+} – in the excited electronic state $2p\sigma$ – possesses a shallow minimum of the total energy E_{tot} [7] and that the same holds for LiH^{3+} in the state $3d\sigma$ [1], the corresponding expectation values $\overline{E_{\text{kin}}}$ and $\overline{E_{\text{pot}}}$ (and E_{tot}) have been computed for a number of internuclear distances R (Tables 2 and 3), and have been plotted in Figs. 3 and 4. Constants

Table 2
System: HeH^{2+} $Z_1 = 2$ $Z_2 = 1$ ($Q = 0$)
State: $2p\sigma$

R	$\overline{E_{\text{kin}}}$	$\overline{E_{\text{pot}}}$	E_{tot}	\bar{z}	$\overline{q^2}$	\bar{q}
0	9/8			0	4/3	8/3
0.1	1.134014	17.737983	18.871997	0.03325	1.32592	2.64826
0.2	1.161062	7.701915	8.862977	0.06599	1.30408	2.59429
0.5	1.333772	1.468475	2.802247	0.15812	1.17381	2.27747
1.0	1.558875	– 0.897227	0.661658	0.30869	0.98262	1.78338
2.0	1.066219	– 1.411405	– 0.345186	0.67499	1.14973	1.77180
3.0	0.679167	– 1.191323	– 0.512157	0.99152	1.52219	2.65202
4.0	0.521178	– 1.052259	– 0.531081	1.34510	1.84743	4.69589
5.0	0.467233	– 0.989775	– 0.522543	1.82964	2.04725	8.35111
6.0	0.462695	– 0.975209	– 0.512514	2.45679	2.10267	13.91685
8.0	0.486780	– 0.989920	– 0.503141	3.77604	2.03214	29.31568
10.0	0.496235	– 0.997272	– 0.501037	4.89584	2.00052	48.12737
12.0	0.498495	– 0.998959	– 0.500464	5.93424	1.99670	70.49236
15.0	0.499432	– 0.999616	– 0.500184	7.45920	1.99727	111.30396

Table 3
System: LiH³⁺ $Z_1 = 3$ $Z_2 = 1$ ($Q = 0$)
State: $3d\sigma$

R	\bar{E}_{kin}	\bar{E}_{pot}	E_{tot}	\bar{z}	$\bar{\varrho}^2$	\bar{q}
0	8/9			0	15/4	9/2
0.1	0.889909	28.220864	29.110772	0.02498	3.74531	4.49823
0.2	0.893012	13.216733	14.109745	0.04986	3.73115	4.49280
0.5	0.916626	4.185552	5.102177	0.12276	3.62936	4.44908
1.0	1.025461	1.044546	2.070007	0.23046	3.24025	4.22802
2.0	1.426602	— 1.009607	0.416995	0.36315	2.06751	3.52037
3.0	1.314788	— 1.508115	— 0.193327	0.59013	1.61874	4.37981
4.0	0.945628	— 1.374466	— 0.428838	1.20240	1.58972	6.80842
5.0	0.648061	— 1.147458	— 0.499397	1.94650	1.75760	9.97845
6.0	0.521950	— 1.033765	— 0.511815	2.53836	1.94176	14.28454
7.0	0.485132	— 0.995133	— 0.510001	3.10758	2.03435	20.34688
8.0	0.481380	— 0.987861	— 0.506481	3.69394	2.05009	28.07055
10.0	0.491244	— 0.993685	— 0.502441	4.83269	2.01862	47.03384
12.0	0.496381	— 0.997457	— 0.501076	5.89710	2.00279	69.67322
15.0	0.498685	— 0.999103	— 0.500418	7.43788	1.99852	110.68798

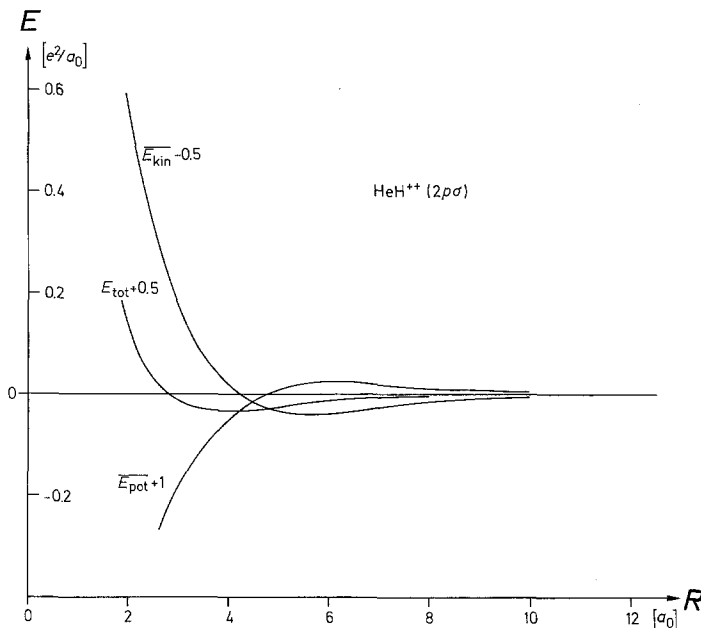


Fig. 3. Expectation values of kinetic and potential energy and eigenvalue E_{tot} as functions of R , for the first excited state $2p\sigma$ of HeH^{++}

have been added to each kind of energy so that each curve goes to zero at infinite separation.

It is evident from Figs. 3 and 4 that Slater's distinction of three ranges of R is valid also for HeH^{2+} ($2p\sigma$) and LiH^{3+} ($3d\sigma$). When R decreases from infinity,

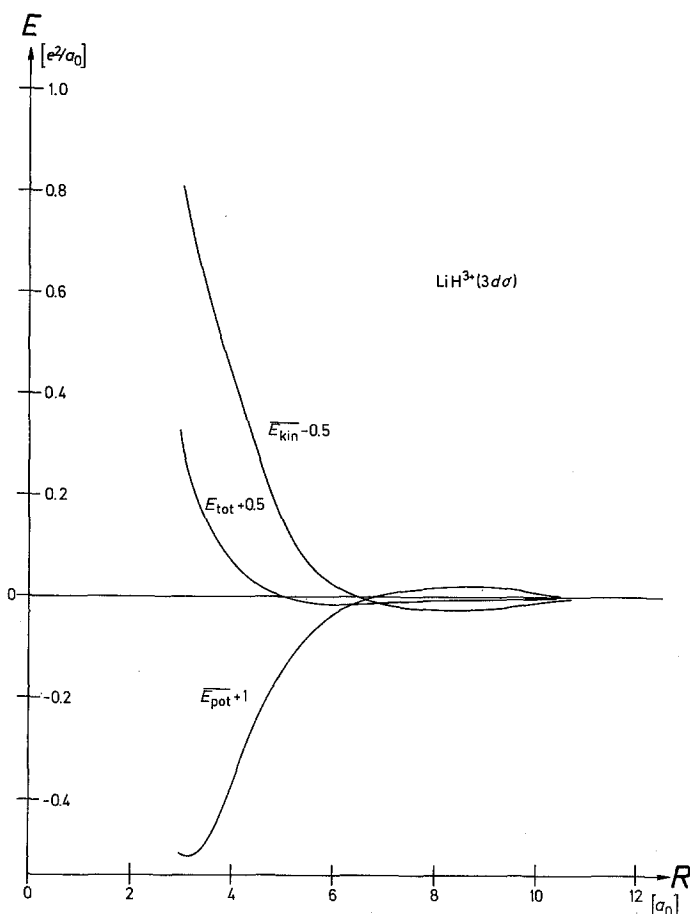


Fig. 4. Expectation values of kinetic and potential energy and eigenvalue E_{tot} as functions of R , for the excited state $3d\sigma$ of LiH^{3+}

the potential energy $\overline{E_{\text{pot}}}$ rises, and the kinetic energy $\overline{E_{\text{kin}}}$ falls ($R > 6a_0$ for HeH^{2+} and $R > 9a_0$ for LiH^{3+}). When R is reduced further, the potential energy is lowered (whereas $\overline{E_{\text{kin}}}$ increases) until it reaches a minimum ($2 < R < 6$ for HeH^{2+} and $3 < R < 9$ for LiH^{3+}). Within this range of R , E_{tot} has its minimum where the decrease of $\overline{E_{\text{pot}}}$ (compared with its value at infinite separation) is only half compensated by the increase of $\overline{E_{\text{kin}}}$. The third range of R is characterized by increasing $\overline{E_{\text{pot}}}$ (due to internuclear repulsion) if R is lowered.

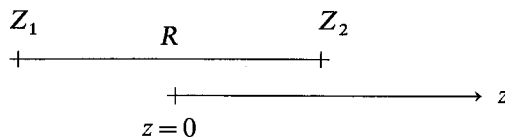
D. Calculation of Dipole Moment Function

For a lot of charge ratios $Z_1 : Z_2$, $Z_1 + Z_2$ being constant and equal to 1, the expectation value \bar{z} of the coordinate z in the electronic state $1s\sigma$ has been computed. Numerical values of the quantity $\bar{z} \cdot Z$, where $Z = Z_1 + Z_2$, as a function of the product RZ , are given in Table 4. Our results agree with those of Moisewitsch

Table 4. Dipole moment function $-\bar{z}Z$
State: $1s\sigma$

$RZ \backslash \lambda$	0.2 LiHe ⁴⁺	1/3 HeH ²⁺	0.5 LiH ³⁺	2.0 (Li, -1) ⁺	3.0 (He, -1)
0.1	0.01004	0.01672	0.02507	0.09890	0.14565
0.2	0.02026	0.03374	0.05051	0.19207	0.26951
0.5	0.05336	0.08849	0.13148	0.41492	0.47733
1.0	0.12095	0.19847	0.28901	0.65843	0.65054
2.0	0.32280	0.51130	0.70170	1.08414	1.06045
3.0	0.64384	0.96094	1.21964	1.54501	1.52972
4.0	1.10924	1.52146	1.78327	2.02674	2.01720
5.0	1.70811	2.13093	2.34589	2.51744	2.51113
6.0	2.38057	2.73466	2.89163	3.01221	3.00776
8.0	3.68556	3.86260	3.94136	4.00691	4.00438
10.0	4.83217	4.91851	4.96350	5.00443	5.00281
12.0	5.89477	5.94540	5.97497	6.00308	6.00195
15.0	7.43623	7.46574	7.48410	7.50197	7.50125
20.0	9.96489	9.98091	9.99109	10.00111	10.00070

and Stewart [8] within the accuracy claimed by these authors. The following orientation of the z -axis, however, has been accepted for Table 4:



Z_1 usually being positive and larger than Z_2 , \bar{z} turns out to be negative. The numerical results have been plotted in Figs. 5 and 6. Fig. 5 gives $-\bar{z} \cdot Z$ directly as a function of the quantity

$$\lambda = \frac{Z_1 - Z_2}{Z_1 + Z_2}$$

introduced by Chang and Byers-Brown [9]. Parameter of each curve is RZ . From the numerical values or from Fig. 5 it can be taken that, for small values of λ , $-\bar{z} \cdot Z$ is nearly proportional to that quantity, RZ being a constant. In general, $\bar{z} \cdot Z$ is an odd function of λ .

In Fig. 6, the dipole moment function $\bar{z}' \cdot Z = \bar{z} + R/2 \cdot Z$ (referring to centre 1 as origin for z') has been plotted against RZ using two logarithmic scales. For small values of RZ , $\bar{z}' \cdot Z$ is nearly proportional to RZ , λ being a constant. So the resulting curves are initially straight lines forming an angle of 45° with the RZ -axis. Inspection of Table 4 shows that, for small values of RZ , indeed

$$\bar{z}Z \approx -\frac{1}{2}\lambda \cdot RZ \quad \text{or} \quad \frac{\bar{z}}{R} \approx \frac{-\lambda}{2}. \quad (12a)$$

The corresponding relations for $z' = z + R/2$ are:

$$\bar{z}'Z \approx \frac{1}{2}(1-\lambda)RZ \quad \text{or} \quad \frac{\bar{z}'}{R} \approx \frac{1}{2}(1-\lambda). \quad (12b)$$

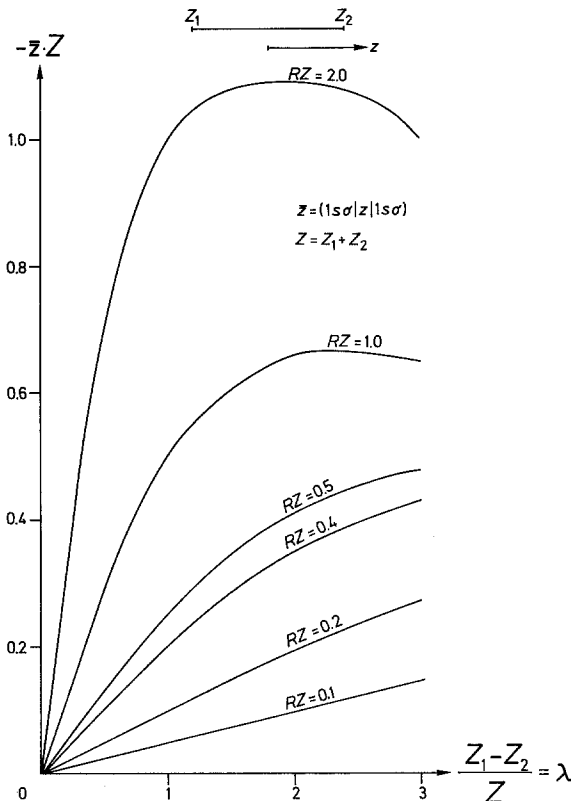


Fig. 5. Expectation value of the centre of negative charge \bar{z} as a function of the ratio $\frac{Z_1 - Z_2}{Z_1 + Z_2}$, for the ground state $1s\sigma$

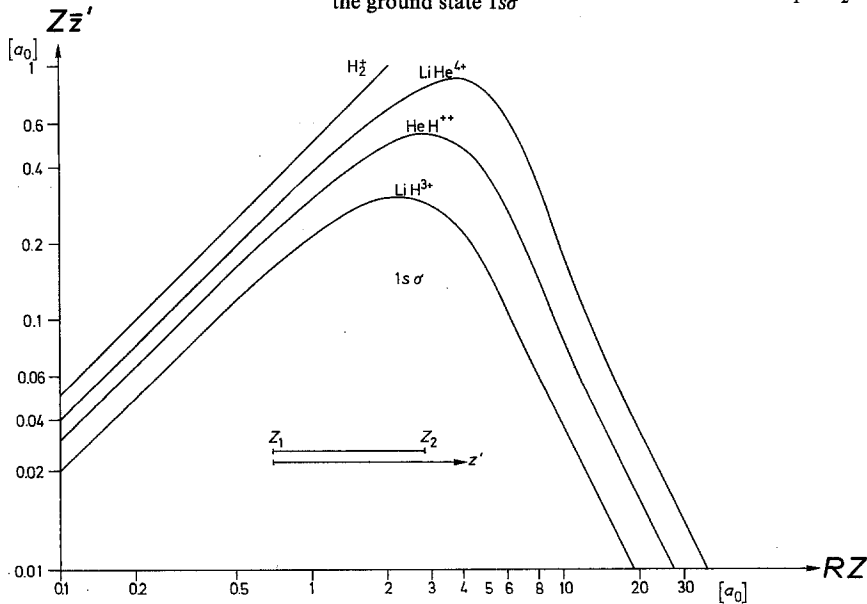


Fig. 6. Expectation value of z' as a function of R for $1s\sigma$ ($z' = 0$ for centre 1)

Table 5. Dipole moment function $\bar{z}'' \cdot Z$ for small values of RZ
State: $1s\sigma$

λ	0.2 LiHe ⁴⁺	1/3 HeH ⁺⁺	0.5 LiH ³⁺	2.0 (Li, -1) ⁺	3.0 (He, -1)	
RZ	$\lambda(\lambda^2-1)$	-0.192	$-\frac{8}{27} = -0.296$	-0.375	6	24
0.01	$-3.8_{10}-8$	$-5.9_{10}-8$	$-7.4_{10}-8$	$1.19_{10}-6$	$4.8_{10}-6$	
0.02	$-3.02_{10}-7$	$-4.66_{10}-7$	$-5.90_{10}-7$	$9.44_{10}-6$	$3.77_{10}-5$	
0.05	$-4.61_{10}-6$	$-7.11_{10}-6$	$-9.00_{10}-6$	$1.44_{10}-4$	$5.73_{10}-4$	
0.10	$-3.54_{10}-5$	$-5.46_{10}-5$	$-6.91_{10}-5$	$1.10_{10}-3$	$4.35_{10}-3$	
0.20	$-2.62_{10}-4$	$-4.04_{10}-4$	$-5.11_{10}-4$	$7.93_{10}-3$	$3.05_{10}-2$	
0.50	$-3.36_{10}-3$	$-5.16_{10}-3$	$-6.48_{10}-3$	$8.51_{10}-2$	$2.73_{10}-1$	
1.00	$-2.09_{10}-2$	$-3.18_{10}-2$	$-3.90_{10}-2$	$3.42_{10}-1$	$8.49_{10}-1$	

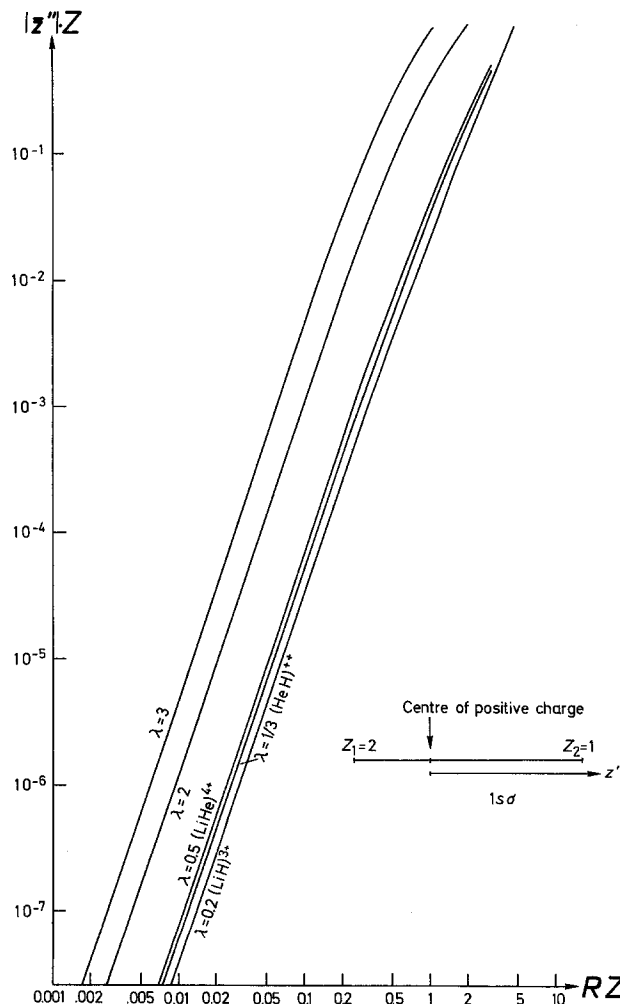


Fig. 7. Expectation value of $z'' = z - z_+$ as a function of R for $1s\sigma$ ($z'' = 0$ for the centre of positive charge)

\bar{z}' vanishes for $\lambda = 1$ and all RZ because then positive charge is only at centre 1. If RZ is increased, $\bar{z}'Z$ remains finite (except for H_2^+) and finally decreases proportional to the inverse square of RZ , as was deduced by Dalgarno and Stewart [10]. Again this asymptotic behaviour is well reflected in Fig. 6.

The relations (12a) and (12b) show that the centre of negative charge \bar{z} approximately coincides with the centre of positive charge

$$z_+ = -\frac{\frac{R}{2}Z_1 + \frac{R}{2}Z_2}{Z_1 + Z_2} = -\frac{1}{2}\frac{Z_1 - Z_2}{Z_1 + Z_2}R = -\frac{1}{2}\lambda R.$$

It is therefore instructing to study also the expectation value of $z'' = z - z_+$, i.e. the dipole moment function with reference to a coordinate system x, y, z' , the origin of which is the centre of positive charge. Expectation values of z'' , as a function of R , are given in Table 5 and have been represented in Fig. 7. We take from our results that, for small values of R , approximately

$$\bar{z}''Z = 0.2\lambda(\lambda^2 - 1)(RZ)^3 \quad (\text{in atomic units}). \quad (13)$$

The polynomial factor $P_3(\lambda) = \lambda(\lambda^2 - 1)$ indicates that the centre of negative charge and that of positive charge coincide for one-electron atomic ions ($\lambda = 1, -1$) and for homonuclear one-electron molecular ions ($\lambda = 0$).

E. Calculation of Quadrupole Moment Functions

Besides of \bar{z} , the expectation values of $\varrho^2 = x^2 + y^2$ and z^2 have been computed, which combined give the expectation value of the quadrupole moment operator

$$q = 3z^2 - r^2 = 2z^2 - \varrho^2 \quad (\text{Table 6}). \quad (14a)$$

Table 6. *Quadrupole moment function $\bar{q} \cdot Z^2$*

State: $1s\sigma$

$RZ \setminus \lambda$	0 H_2^+	0.2 LiHe $^{4+}$	0.3 HeH $^{2+}$	0.5 LiH $^{3+}$	2.0 (Li, -1) $^+$	3.0 (He, -1)
0.1	0.00167	0.00180	0.00204	0.00251	0.01474	0.03013
0.2	0.00669	0.00724	0.00820	0.01008	0.05623	0.10566
0.5	0.04251	0.04621	0.05270	0.06506	0.27868	0.36923
1.0	0.17666	0.19477	0.22562	0.28125	0.77607	0.77983
2.0	0.77380	0.88853	1.06590	1.33713	2.29156	2.22079
3.0	1.91650	2.31838	2.84414	3.48177	4.74346	4.66786
4.0	3.75481	4.80283	5.86123	6.84704	8.19934	8.13228
5.0	6.46219	8.65446	10.22120	11.37667	12.66609	12.60827
6.0	10.22777	14.00229	15.82268	16.97332	18.14144	18.09133
8.0	21.65131	28.59039	30.22274	31.17502	32.10833	32.06931
10.0	38.98401	47.27945	48.55127	49.32313	50.08748	50.05574
12.0	62.03581	69.74905	70.78057	71.42809	72.07327	72.04659
15.0	105.23198	110.69569	111.51387	112.03695	112.55885	112.53735
20.0	195.79622	198.63535	199.25268	199.64926	200.04427	200.02806

It is, however, more instructive to plot the expectation value of the quadrupole moment q' referring to centre 1 of the coordinate system, as this quantity remains finite (except for H_2^+):

$$q' = 3z'^2 - r_1^2 = 2z'^2 - \varrho'^2. \quad (14b)$$

As $\varrho = \varrho'$ and $z' = z + R/2$, the two moments q and q' are linked by the relation

$$q' = q + 2R\bar{z} + R^2/2. \quad (15)$$

In Fig. 8, $Z^2 \bar{q}'$ is plotted against RZ using logarithmic scales. For small values of RZ , $Z^2 \bar{q}'$ is proportional to the square of RZ resulting in an ascending straight line. A further inspection of the numerical values (Table 6) leads to the conclusion that

$$Z^2 \bar{q}' \approx \frac{1}{3}(1 - \lambda)(2 - \lambda)(RZ)^2 \quad \text{for small values of } RZ. \quad (16)$$

It is not surprising that the quadrupole moment vanishes for $\lambda = 1$ and all RZ , in this case no charge being at centre 2. But it is striking that this vanishing occurs also for $\lambda = 2$ which means, for instance, 3 positive unit charges at centre 1 and one negative unit charge at centre 2. However, there is no complete vanishing, higher powers of RZ becoming essential.

For large values of RZ , $Z^2 \bar{q}'$ is proportional to the inverse third power of RZ (Dalgarno and Stewart [10]). Again this behaviour is nicely shown in Fig. 8.

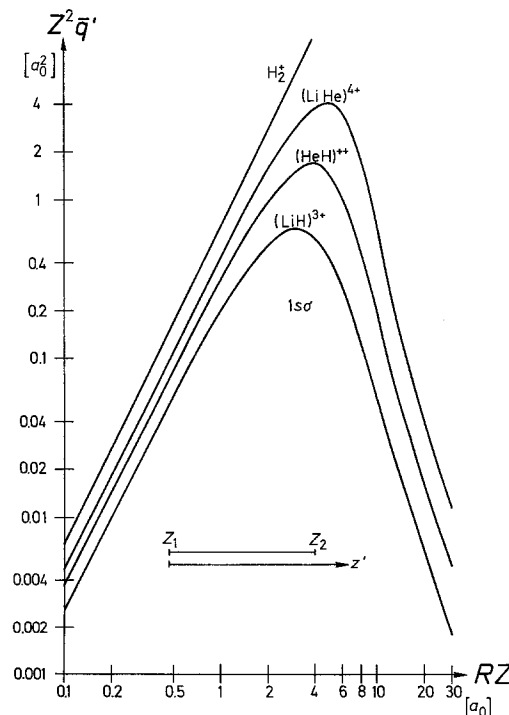


Fig. 8. Expectation value of $3z'^2 - r^2$ as a function of R , for $1s\sigma$

F. Some Properties of Those Generalized Diatomic Orbitals Which Approach Slater-Zener Type Orbitals for $R \rightarrow 0$

Be Q a constant independent of R . Generalized diatomic orbitals in which

i) the number of nodes of $U(\mu)$ is zero (i.e. $n_r = n_\mu = S = 0$)

ii) $Q = -\frac{1}{2}(n^*(n^* - 1) - l(l + 1))$ in Eq. (1)

converge, for $R \rightarrow 0$, to Slater-Zener type functions (STAOS)

$$\chi_0 = N r^{n^*-1} e^{\frac{-Zr}{n^*}} Y_l^m(\theta, \varphi) \quad (17)$$

where N is a normalization constant, $Z = Z_1 = Z_2$, and the corresponding electron energy is

$$E_0 = -\frac{Z^2}{2n^{*2}} \quad [11]. \quad (18)$$

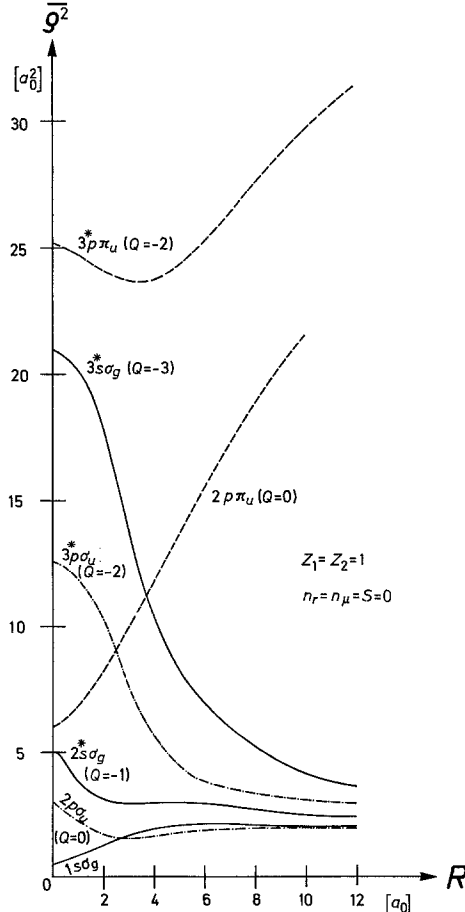


Fig. 9. Expectation values of $\varrho^2 = x^2 + y^2$ as functions of R , for some Slater-type diatomic orbitals $|n^*l\gamma\rangle$

For $R \rightarrow \infty$, they converge to a linear combination of two atomic orbitals $|0\,Tm\rangle$ centered at centre 1 respectively 2 ($Z_1 = Z_2$) or to one atomic orbital $|0\,Tm\rangle$ centered either at centre 1 or at centre 2 [1]. As a consequence, all generalized diatomic orbitals $|n^*lm\rangle$ of the type characterized above which agree in l and m have the same limit function for $R \rightarrow \infty$. Therefore all expectation values tend to become equal for $R \rightarrow \infty$ within each of the following three groups of functions:

- a) $l = m = 0$
 $1s\sigma_g(Q=0), 2^*s\sigma_g(Q=-1), 3^*s\sigma_g(Q=-3)$
- b) $l = 1, m = 0$
 $2p\sigma_u(Q=0), 3^*p\sigma_u(Q=-2)$
- c) $l = m = 1$
 $2p\pi_u(Q=0), 3^*p\pi_u(Q=-2)$.

This behaviour is shown in Fig. 9, in which $\overline{\varrho^2}$ is plotted against R for these three groups of functions, assuming $Z_1 = Z_2 = 1$.

The limit $\overline{\varrho_0^2}$ for $R = 0$ can easily be computed:

As $\varrho_0^2 = r_0^2 \sin^2 \theta$ and as $\sin^2 \theta = \frac{2}{3}(P_0(\cos \theta) - P_2(\cos \theta))$, we get

$$\overline{\varrho_0^2} = \overline{r_0^2} \cdot \frac{2}{3}(1 - c^2(lm, lm)), \quad (19)$$

where the numerical value of $c^2(lm, lm)$ may be found in the book by Condon and Shortley [12, p. 175]. From the same authors [12, p. 117] we take that

$$\overline{r_0^2} = \frac{1}{2} [5n^2 + 1 - 3l(l+1)] \frac{n^2 a_0^2}{Z^2} \quad (20a)$$

for hydrogenic orbitals.

For Slater orbitals,

$$\overline{r_0^2} = \frac{1}{2} [2n^{*2} + 3n^* + 1] \frac{n^{*2} a_0^2}{Z^2}, \quad (20b)$$

Table 7

System: $Z_1 = Z_2 = 1 \quad Q = -1$
State: $2^*s\sigma_g$ converging to Slater orbital 2^*s with $Z = 2$
 $(n_r = n_\mu = S = 0)$

R	$\overline{E_{\text{kin}}}$	$-\frac{1}{r_1} - \frac{1}{r_2}$	$\frac{1}{r_1 \cdot r_2}$	$\overline{E_{\text{pot}}}$	E	$\overline{\varrho^2}$	\bar{q}
0	1/6	-1	1/3	-2/3	-1/2	5	0
0.1	0.1667	-1.0022	0.3350	-0.6672	-0.5006	4.9851	0.0027
0.2	0.1668	-1.0089	0.3398	-0.6691	-0.5022	4.9406	0.0106
0.5	0.1712	-1.0541	0.3692	-0.6849	-0.5137	4.6478	0.0652
1.0	0.1990	-1.1740	0.4266	-0.7474	-0.5484	3.8886	0.2479
2.0	0.2554	-1.2325	0.3776	-0.8549	-0.5995	3.0181	0.9782
3.0	0.2614	-1.1256	0.2706	-0.8550	-0.5936	2.9318	2.4465
4.0	0.2650	-1.0355	0.2015	-0.8340	-0.5690	2.9999	5.0274
5.0	0.2820	-0.9888	0.1612	-0.8275	-0.5456	3.0152	9.0692
6.0	0.3096	-0.9749	0.1367	-0.8381	-0.5285	2.9391	14.7069
8.0	0.3658	-0.9853	0.1081	-0.8772	-0.5114	2.6774	29.9114
10.0	0.4001	-0.9956	0.0897	-0.9058	-0.5058	2.4876	48.8543
12.0	0.4189	-0.9989	0.0764	-0.9225	-0.5036	2.3821	71.2864

which can be deduced from (20a) by putting $n = n^*$ and $l = n^* - 1$, as all Slater orbitals with the same n^* have the same radial part $R_n^*(r)$ which agrees with the hydrogenic radial part $R_{nl}(r)$ for $n = n^*$ and $l = n - 1$.

In Table 7, several expectation values, as functions of R , have been collected which have been computed with the nodeless Slater-type diatomic orbital $2^*s(Z_1 = Z_2, Q = -1)$ converging to the Slater-type atomic function $2^*s(Z = 2)$.

Acknowledgement. The author is indebted to Professor Dr. Hartmann, Professor Dr. Byers-Brown and Priv. Doz. Dr. Schmidke for stimulating this research and to the Deutsche Forschungsgemeinschaft for paying computer time on the CD 3300 of the University of Mainz and on the CD 6600 of Regionales Rechenzentrum im Institut für Statik und Dynamik der Luft- und Raumfahrtkonstruktionen of the University of Stuttgart.

G. Appendix

If (1) is separated in spheroidal coordinates μ, v, φ , the differential equation for $V(v)$ turns out to be

$$\left\{ -\frac{d}{dv} (1-v^2) \frac{d}{dv} + A' + Dv + p^2(1-v^2) + \frac{m^2}{1-v^2} \right\} V(v) = 0. \quad (21)$$

(This is Eq. (5a) of [1]). Here A' is the separation constant, D stands for $RZ_1 - RZ_2$, and p is the energy parameter.

We assume that the following expansion of $V(v)$ in terms of associated Legendre functions of the first kind holds:

$$V(v) = \sum_{k=0}^{\infty} d'_k P_{|m|+k}^{(m)}(v). \quad (22)$$

(21) and (22) give rise to the following linear five-term recursion formula for the coefficients d'_k :

$$B_{k,k-2} d'_{k-2} + B_{k,k-1} d'_{k-1} + (B_{k,k} + A') d'_k + B_{k,k+1} d'_{k+1} + B_{k,k+2} d'_{k+2} = 0. \quad (23)$$

The elements of the pentadiagonal matrix B occurring here are defined by

$$\begin{aligned} B_{k,k-2} &= -\frac{(k-1)k}{(2l-3)(2l-1)} p^2 \quad l = k + |m| \\ B_{k,k-1} &= \frac{k}{2l-1} D \\ B_{k,k} &= 2 \frac{l(l+1)+m^2-1}{(2l-1)(2l+3)} p^2 + l(l+1) \\ B_{k,k+1} &= \frac{l+|m|+1}{2l+3} D \\ B_{k,k+2} &= -\frac{(l+|m|+1)(l+|m|+2)}{(2l+3)(2l+5)} p^2. \end{aligned} \quad (24)$$

References

1. Helfrich, K., Hartmann, H.: *Theoret. chim. Acta (Berl.)* **16**, 263 (1970).
2. Slater, J. C.: *Quantum theory of molecules and solids*, Vol. I, page 34. New York: McGraw-Hill 1963.
3. Hartmann, H., Helfrich, K.: *Theoret. chim. Acta (Berl.)* **10**, 406 (1968).
4. Zurmühl, R.: *Praktische Mathematik*, 4th edition, Berlin: Springer 1964.
5. Olver, F. W. J.: *Math. of Comp.* **18**, 65 (1964).
6. Miller, J.: *Math. of Comp.* **17**, 84 (1963).
7. Bates, D. R., Carson, T. R.: *Proc. Roy. Soc. (London) A* **234**, 207 (1956).
8. Moisewitsch, B. L., Stewart, A. L.: *Proc. physic. Soc. A* **69**, 480 (1956).
9. Chang, T. Y., Byers-Brown, W.: *Theoret. chim. Acta (Berl.)* **4**, 393 (1966).
10. Dalgarno, A., Stewart, A. L.: *Proc. Roy. Soc. (London) A* **238**, 276 (1957).
11. Kehl, S., Helfrich, K., Hartmann, H.: *Theoret. chim. Acta (Berl.)*
12. Condon, E. U., Shortley, G. H.: *The theory of atomic spectra*. Cambridge: University Press 1957.

Dr. K. Helfrich
Institute and Centre of
Theoretical Chemistry
University of Frankfurt
BRD-6000 Frankfurt am Main 1
Robert Mayer-Str. 11
Germany